



Calibrating the TP-AGB phase through resolved stellar populations in the Small Magellanic Cloud

G. Pastorelli¹, P. Marigo¹, L. Girardi², S. Rubele¹, A. Nanni¹, Y. Chen¹, A. Bressan³,
B. Aringer¹, M. Trabucchi¹, J. Montalbán¹, S. Bladh¹, and M.-R. L. Cioni^{4,5}

¹ Dipartimento di Fisica e Astronomia, Università di Padova, Vicolo dell'Osservatorio 3, 35122 Padova, Italy, e-mail: giada.pastorelli@studenti.unipd.it

² Osservatorio Astronomico di Padova, Vicolo dell'Osservatorio 5, 35122 Padova, Italy

³ SISSA, via Bonomea 365, I-34136 Trieste, Italy

⁴ Leibniz-Institut für Astrophysik Potsdam, An der Sternwarte 16, 14482 Potsdam, Germany

⁵ University of Hertfordshire, PAM, College Lane, Hatfield AL10 9AB, United Kingdom

Abstract. The Thermally-Pulsing Asymptotic Giant Branch (TP-AGB) phase is one of the most uncertain evolutionary phase of low- and intermediate-mass stars. The classical calibration based on Magellanic Clouds (MCs) clusters has proved to be unsuitable for other galaxies and the overall contribution of TP-AGB stars to the integrated light of galaxies is still a matter of debate. The high-quality observations of resolved populations in the MCs offer a unique opportunity to extend and enhance the calibration of this phase. We constrain the key uncertain parameters by comparing observed star counts, luminosity functions and color distributions of the TP-AGB population in the Small Magellanic Cloud (SMC) with those computed through the stellar population synthesis code TRILEGAL, which includes the latest TP-AGB evolutionary tracks from the COLIBRI code. The strength of our approach is represented by the detailed space-resolved star formation history of the SMC, derived from the deep near-infrared photometry of the VISTA survey of the MCs.

Key words. Stars: AGB – Stars: mass-loss – Magellanic Clouds

1. Introduction

The Thermally Pulsing Asymptotic Giant Branch (TP-AGB) is an advanced evolutionary phase during which stars of low- and intermediate-mass ($1-8 M_{\odot}$) experience helium and hydrogen double shell burning, reach their highest luminosities, synthesize new elements, go through mass loss via stellar winds and finally reach the stage of white dwarfs. The impact of this evolutionary phase spans from chemical evolution and spectral energy distri-

bution of galaxies to dust production in galaxies at low and high redshift. Despite its importance in our understanding of galaxy evolution, the TP-AGB modelling is still affected by large uncertainties due to the presence of several and interconnected processes – i.e. Third Dredge-Up (3DU), Hot-Bottom Burning (HBB), stellar winds, long period pulsations, reprocessing of radiation by circumstellar dust – for which a robust theory is still lacking. Large imaging and spectroscopic surveys provided excellent data of AGB stars in regions

with well characterized Star Formation History (SFH), i.e. metal rich fields of M31 from the Panchromatic Hubble Andromeda Treasury (PHAT) survey (Dalcanton et al., 2012), metal-poor dwarf galaxies from the ACS Nearby Galaxy Survey Treasury (ANGST), complete census of AGB stars in the MCs from 2MASS and *Spitzer* surveys (Boyer et al., 2011, SAGE surveys). These data can be compared with the predictions of detailed evolutionary tracks and isochrones (Marigo et al., 2017) to constrain the uncertain parameters of the models as a function of age and metallicity (as done in Girardi et al., 2010; Rosenfield et al., 2014, 2016). In this work, we use the population synthesis code TRILEGAL (Girardi et al., 2005) to produce synthetic samples of TP-AGB stars in the SMC. The predicted star counts, luminosity functions (LFs), color distributions are compared to the observed ones from the AGB candidate list by Srinivasan et al. (2016, SR16). Our purpose is to put quantitative constraints on lifetimes and efficiency of the critical processes of mass-loss, 3DU and HBB, in addition to the circumstellar dust properties.

2. Data and methods

2.1. Stellar models

The evolution prior to the TP-AGB phase is computed with the PARSEC code (Bressan et al., 2012) and the TP-AGB phase is followed by the COLIBRI code (Marigo et al., 2013). COLIBRI includes the on-the-fly computation of detailed molecular chemistry and opacities (Marigo & Aringer, 2009), it fully accounts for the HBB nucleosynthesis and energetics through a complete nuclear network coupled to a diffusive description of convection. Given the uncertainties in the mass-loss and 3DU, these processes are treated with a parametrised description. The resulting free parameters (occurrence and efficiency of 3DU, mass-loss prescription) can be tuned to reproduce the observations. For any combination of input prescriptions, the code allows a very quick computation of large grids of tracks. Such a feature makes COLIBRI a suitable tool for the calibration cycle.

2.2. Star Formation History

The SFH is computed with a CMD-fitting technique which relies on the deep near-IR photometry of the VISTA survey of the MCs (VMC, Cioni et al., 2011). These data reached the oldest main-sequence turn-off points, ensuring a robust measurement of the Star Formation Rate (SFR) and Age-Metallicity Relation (AMR), in addition to distance and reddening. Rubele et al. (2015) derived the SFH for a 14-deg² area of the SMC, split into 120 subregions, including its main body and wing. In this work, we used a revised version of the SFH; the main improvements being the use of the latest version of PARSEC tracks, a better estimate of distance and reddening, and deeper photometry (Rubele et al., in prep).

2.3. AGB stars in the SMC

SR16 identified and classified the population of TP-AGB stars using NIR and MIR colors (Boyer et al., 2011). The catalog includes the 81 Spitzer IRS sources spectroscopically classified by Ruffle et al. (2015). We included the spectroscopic classification of 273 sources analyzed by Boyer et al. (2015). The resulting catalog contains optical to far-IR photometry of ≈ 5700 AGBs classified in Oxygen-rich (O-AGB), Carbon-rich (C-AGB), anomalous-AGB (a-AGB) and extreme (x-AGB).

2.4. Population synthesis

The TP-AGB population of each VMC subregion is modeled with TRILEGAL, according to its SFH, distance and reddening. Given the accuracy of the SFH, we directly derived the total stellar mass of each region by integrating the SFR over the age values, instead of adopting normalization factors based on number counts. The stellar spectral libraries for C- and O-rich giants are based on the COMARCS atmosphere models by Aringer et al. (2009, 2016). The dust bolometric corrections are based on the model of condensation and growth of dust grains by Nanni et al. (2013, 2016). The resulting stellar catalogs are merged together in a single catalog

with stellar parameters and synthetic photometry. According to their C/O ratio, the synthetic TP-AGB stars are separated in C- and O-AGB stars. The x-AGB stars are selected by the photometric criteria used by Boyer et al. (2011). To allow a direct comparison with the observations, we assigned the sources identified by SR16 to the correspondent VMC region, according to their sky position, and we only considered those VMC regions completely covered by the AGB catalog.

3. Results

We are currently exploring the effects of different prescriptions for the onset and efficiency of the 3DU and different mass-loss prescriptions from the literature. Here we show some examples obtained with four sets of models. The starting model (S1) is computed with the evolutionary tracks described in Marigo et al. (2017). The mass-loss prescription for the pre-dust driven wind is a modified version of the Schröder & Cuntz (2005, SC05) prescription (Rosenfield et al., 2016). During the dust-driven wind phase we adopt a formalism similar to Bedijn (1988). The mass-loss prescription in model S2 is from Bloeker (1995, BL95) with an efficiency parameter $\eta=0.4$ and it is applied for both the pre-dust and dust-driven regimes. Model S3 has a less efficient mass-loss (BL95 with $\eta=0.02$) and a delayed onset¹ of the 3DU. In model S4 we adopt the modified SC05 prescription for the pre-dust regime and the BL95 with $\eta=0.02$ for the dust-driven phase. In Figure 1 we compare the observed and synthetic Ks-band LFs. The results are shown for the whole AGB population and for O-AGB, C-AGB and x-AGB separately. The total number counts and the χ^2 for each class are also shown. The total number of AGB stars is reproduced within $\approx 20\%$ with model S1, but we find an excess of O-AGB by $\approx 50\%$ and a deficit of C-AGB stars by $\approx 30\%$. As expected, the high efficiency of the mass-loss adopted in model S2 results in an underproduction of AGB stars ($\approx 40\%$). Model S3

¹ The value of the minimum core-mass for 3DU to occur is reduced by $0.02 M_{\odot}$ with respect to Karakas et al. (2002) for all values of initial mass.

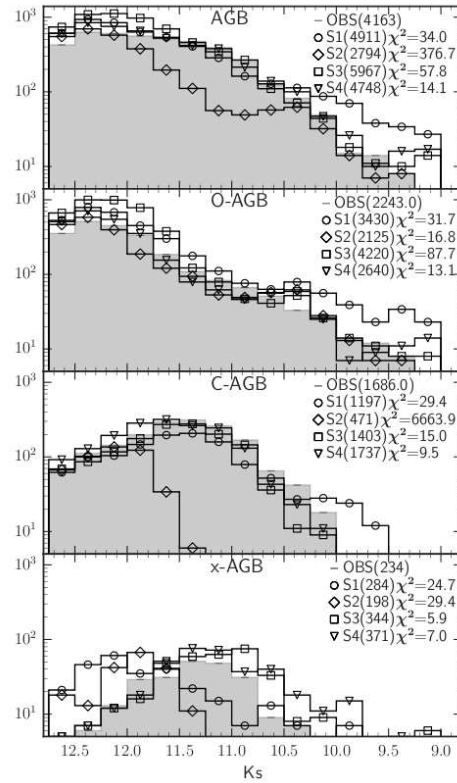


Fig. 1. Observed (grey area) and synthetic Ks-band LFs of models S1, S2, S3, S4 (circles, diamonds, squares, and triangles). The LFs are computed for the whole AGB population and for the O-, C- and x-AGB separately. The total number counts is shown in parenthesis. The value of the χ^2 is also shown.

gives better result for the C-AGB, but the O-AGB are overestimated by the $\approx 90\%$. The observations are better reproduced by model S4. In this case, the total number counts are reproduced within $\approx 15\%$ and the number counts of O- and C-AGB within $\approx 18\%$ and $\approx 4\%$ respectively. Figure 2 shows the J-Ks vs. Ks-3.6 μm Color-Color Diagram (CCD) of the observed a-, C and x-AGB stars and the synthetic C- and x-AGB of model S4. The observed distribution is nicely reproduced by this model, in which we adopt the Rouleau & Martin (1991) optical dataset for C-dust, with typical grain size $\approx 0.1 \mu\text{m}$ (Nanni et al., 2016).

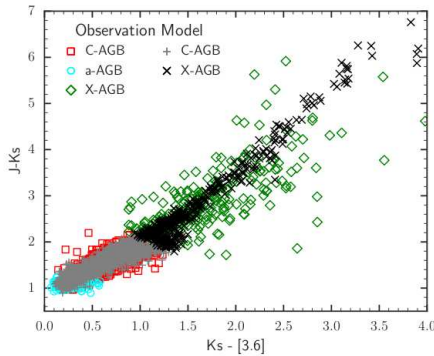


Fig. 2. J-Ks vs. Ks-3.6 μ m CCD of observed a-, C and x-AGB (cyan circles, red squares, green diamonds) and synthetic C- and x-AGB (grey pluses, black crosses) from model S4.

4. Conclusions

We presented some preliminary results of the on-going calibration of TP-AGB models computed with the COLIBRI code. The best-fit model reproduces the observed number counts within $\approx 15\%$. The inclusion of the revised dust-formation model by Nanni et al. (2016) allows to reproduce the color distributions of C- and x-AGB stars. Our aim is to reproduce several SMC observables at the same time (star counts, LFs, color distributions, pulsation periods), hence to shed light on critical aspects of the evolution of TP-AGB stars. The calibration will be extended to the Large Magellanic Cloud and other nearby systems i.e. M33, M31 and MCs clusters (Chen et al. in prep.) to probe different areas of the age-metallicity plane. The isochrones presented in Marigo et al. (2017) (model S1), and further updates are available at <http://stev.oapd.inaf.it/cmd> or <http://starkey.astro.unipd.it/cgi-bin/cmd>.

Acknowledgements. We acknowledge the support from the ERC Consolidator Grant funding scheme (project *STARKEY*, G.A. n. 615604). We thank the VMC team for sharing the details of the SFH.

References

- Aringer, B., et al. 2009, *A&A*, 503, 913
 Aringer, B., et al. 2016, *MNRAS*, 457, 3611
 Bedijn, P. J. 1988, *A&A*, 205, 105
 Bloeker, T. 1995, *A&A*, 297, 727
 Boyer, M. L., McDonald, I., Srinivasan, S., et al. 2015, *ApJ*, 810, 116
 Boyer, M. L., Srinivasan, S., van Loon, J. T., et al. 2011, *AJ*, 142, 103
 Bressan, A., Marigo, P., Girardi, L., et al. 2012, *MNRAS*, 427, 127
 Cioni, M.-R. L., Clementini, G., Girardi, L., et al. 2011, *A&A*, 527, A116
 Dalcanton, J. J., Williams, B. F., Melbourne, J. L., et al. 2012, *ApJS*, 198, 6
 Girardi, L., et al. 2005, *A&A*, 436, 895
 Girardi, L., Williams, B. F., Gilbert, K. M., et al. 2010, *ApJ*, 724, 1030
 Karakas, A. I., Lattanzio, J. C., & Pols, O. R. 2002, *PASA*, 19, 515
 Marigo, P. & Aringer, B. 2009, *A&A*, 508, 1539
 Marigo, P., et al. 2013, *MNRAS*, 434, 488
 Marigo, P., Girardi, L., Bressan, A., et al. 2017, *ApJ*, 835, 77
 Nanni, A., et al. 2013, *MNRAS*, 434, 2390
 Nanni, A., Marigo, P., Groenewegen, M. A. T., et al. 2016, *MNRAS*, 462, 1215
 Rosenfield, P., Marigo, P., Girardi, L., et al. 2014, *ApJ*, 790, 22
 Rosenfield, P., Marigo, P., Girardi, L., et al. 2016, *ApJ*, 822, 73
 Rouleau, F. & Martin, P. G. 1991, *ApJ*, 377, 526
 Rubele, S., Girardi, L., Kerber, L., et al. 2015, *MNRAS*, 449, 639
 Ruffe, P. M. E., Kemper, F., Jones, O. C., et al. 2015, *MNRAS*, 451, 3504
 Schröder, K.-P. & Cuntz, M. 2005, *ApJ*, 630, L73
 Srinivasan, S., Boyer, M. L., Kemper, F., et al. 2016, *MNRAS*, 457, 2814